Turkish Journal of Electrical Engineering & Computer Sciences

http://journals.tubitak.gov.tr/elektrik/

Research Article

Turk J Elec Eng & Comp Sci
(2016) 24: 3586 – 3596

doi:10.3906/elk-1405-206

Common-mode EMI evaluation of forward converter with various core-reset schemes

Mohammad Rouhollah YAZDANI*, Nahid AMINI FILABADI
Department of Electrical Engineering, Isfahan (Khorasgan) Branch, Islamic Azad University, Isfahan, Iran

Received: 31.05.2014 • **Accepted/Published Online:** 20.05.2015 • **Final Version:** 20.06.2016

Abstract: In switching power converters, electromagnetic emissions can interfere with the normal operation of the converter or other adjacent systems. Among various power converters, forward converters are widely used at low and medium powers that need a transformer core-reset scheme. In this paper, a prediction procedure for conducted common-mode EMI of a single-switch forward converter is presented, and common-mode EMI levels are predicted considering heat-sink parasitic capacitors and main PCB parasitic elements. The accuracy of prediction results is examined via experimental results. In addition, effects of conventional passive core-reset schemes on the conducted EMI are evaluated via experimental results. Along with the passive reset scheme, common-mode EMI of the low-side and high-side active clamps are evaluated. Finally, the EMI comparison between various core-reset techniques is presented.

Key words: Electromagnetic interference, common-mode EMI, core-reset, electromagnetic compatibility, forward converter

1. Introduction

Switching power converters are widely employed in energy conversion systems due to advantages such as high efficiency. However, one of the most important problems in switching converters is electromagnetic interference (EMI) due to high rates of di/dt and dv/dt. The forward converter as a popular switching power converter has been widely used due to its features such as low cost, circuit simplicity, and high efficiency, in addition to capability of multiple outputs via an isolation transformer.

The single-switch forward converter needs additional transformer core-reset schemes to avoid core saturation [1], such as tertiary (reset) winding, zener diode, resistor–capacitor–diode (RCD), and active clamp techniques, as shown in Figures 1a–1e.

The magnetizing inductance energy is recycled to the input source in the forward converter, with reset winding [2] as a main advantage. However, the extra reset winding complicates the transformer construction. Another drawback of the tertiary winding schemes is that the energy stored in the transformer leakage inductance during switch turn-on is not recovered, leading to a high voltage spike across the main switch. Zener diode and RCD clamp circuits absorb the magnetizing inductor energy and discharge the leakage inductance. Thus, the main switch has considerably lower voltage spike and stress than with the reset winding circuit. The zener diode and RCD clamps are simple and cost-effective reset solutions. However, their disadvantages are the energy dissipation of the magnetizing and leakage inductances, and converter efficiency degradation [3]. On the other hand, the reset process is nearly lossless via an active clamp circuit, which recycles the transformer energy to

*Correspondence: m.yazdani@khuisf.ac.ir

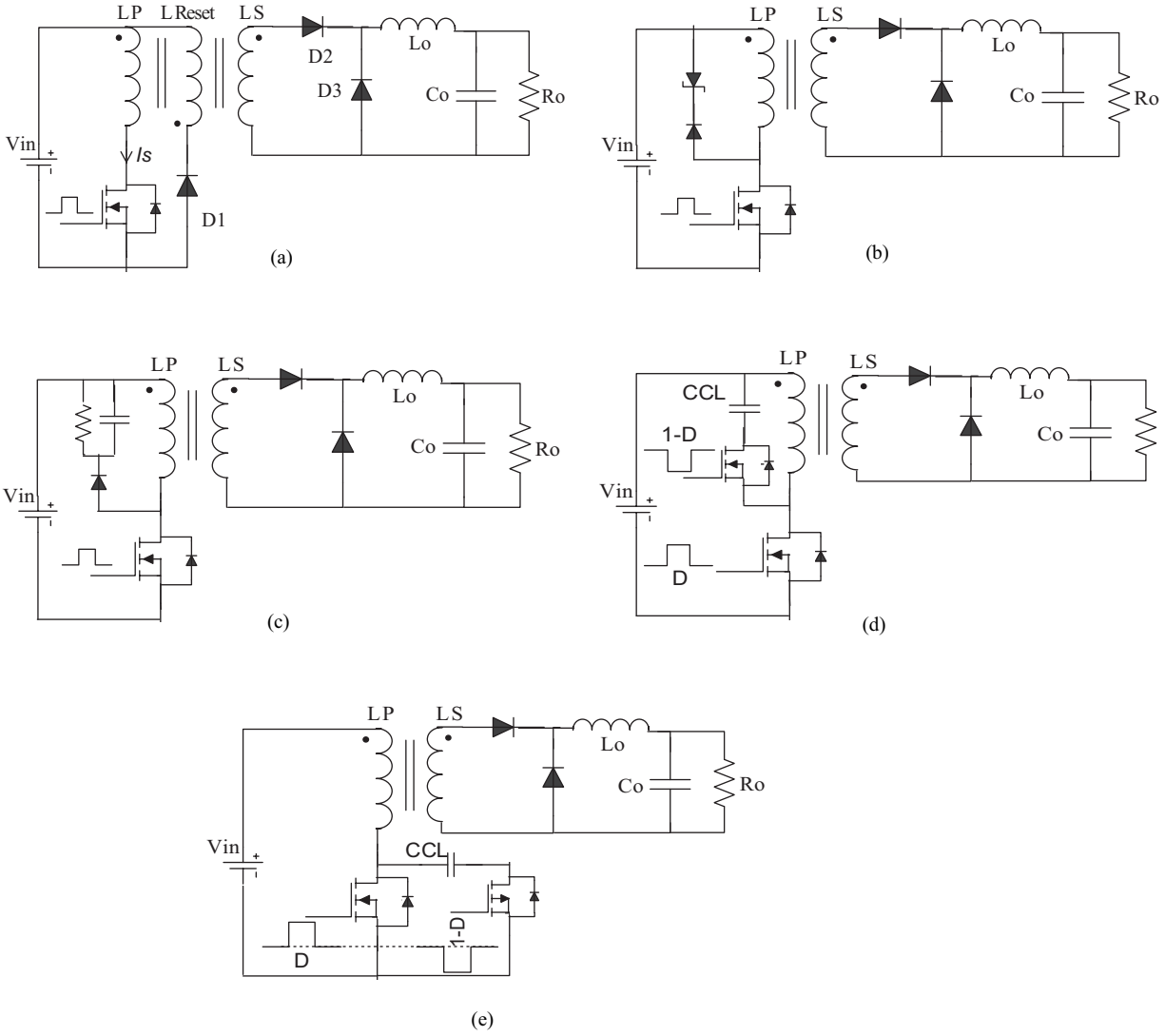

Figure 1. Single-switch forward converter with various reset schemes: a) reset winding; b) zener diode clamp; c) RCD clamp; d) high-side active clamp; e) low-side active clamp.

the input source [4]. Core-reset via active schemes yields the possibility of a duty cycle above 50% and lower voltage stress than conventional passive schemes [5]. The transformer core is reset at a lower voltage via active clamp techniques during the whole turn-off time with respect to other reset methods, in which the transformer core would reset at a higher voltage during a short time. However, the cost and parasitic elements can be increased in the active clamp circuits due to using a capacitor, a switch, and its gate driver.

Some inherent concerns of the forward converter with various reset schemes such as switch stress, voltage conversion ratio, core saturation, and losses have been studied in the previous literature [1–7]. However, there is a lack of modeling and practical analysis of common-mode EMI in the forward converter via evaluation of passive and active core-reset schemes. To model the EMI, the frequency domain or time domain can be used [8]. The frequency domain approach utilized in several papers is based on the equivalent noise source and propagation path concept. Although the prediction process is reduced with respect to the time domain method, this method has some assumptions, such as considering an ideal model for noise sources [9], and may

provide little information about some key circuit parameters for compliance with EMC standards. On the other hand, the time domain approach dominates all parasitic parameters separately and includes resonant frequencies caused by parasitic components and coupling paths, leading to more accurate EMI prediction than the frequency domain method. In this paper, time domain analysis is proposed to predict common-mode (CM) electromagnetic emissions in the isolated forward converter, due to the complexity of EMI phenomena in the forward topology.

This paper is organized as follows. In Section 2, the procedure of CM-EMI modeling is proposed. The CM-EMI prediction results are shown for a forward converter. CM-EMI experimental results are presented for a forward converter with reset winding in Section 3 to examine the prediction results. Since conducted EMI depends on circuit topology and its parasitic elements and varies by changing core-reset schemes, CM-EMI levels of forward converter with mentioned core-reset schemes are compared in Section 4 via experimental results to evaluate the proper reset method from the EMI standpoint. In Section 5, concluding remarks are drawn.

2. Common-mode EMI prediction

Electromagnetic compatibility (EMC) organizations, such as the Special Committee on Radio Interference (CISPR) [10] and the Federal Communications Commission (FCC), set limits and standards on the amounts of radiated and conducted electromagnetic emissions Since satisfying EMC standards after building the switching converter is costly and time-consuming, proper modeling of EMI including noise sources and propagation paths is necessary in the design stage.

2.1. Converter EMI modeling

EMI modeling in the first step of design would assist designers in predicting electromagnetic emissions before final realization [11]. Conducted electromagnetic emissions can be divided into differential-mode (DM) [12] and common-mode (CM) [13]. The CM current passes through parasitic components between the converter elements and earth (chassis). Several papers focus on CM-EMI in nonisolated converters [12]. CM-EMI is a result of the current and voltage pulsating generated by high-frequency switching [13]. Since the input pulsating current occurs at buck topologies such as the isolated forward converter, the CM-EMI would be important as considered in this paper.

In this paper, an isolated 50 W regular forward converter was designed with input voltage of 48 V_{DC}, 33% duty cycle (D), and 130 kHz switching frequency (f_{sw}) [14] to examine its CM-EMI. The reset technique is the tertiary winding method shown in Figure 1a, and the turn ratio of the primary and reset windings is almost unity. The realized transformer specification and main converter components are summarized in Table 1.

Table 1. Main components of forward converter.

Main switch	IRF840
Diodes	MUR860
L_P, R_P	139 mu H, 61 mΩ
L_{Reset}, R_{Reset}	136 mu H, 60 mΩ
L_S, R_S	88 mu H, 12 mΩ
Cross-coupling capacitances	˜16 to 21 pF
Output choke	80 mu H
Output capacitor	100 mu F

The prediction procedure is based on time domain simulation and fast Fourier transform (FFT) analysis. However, the time domain method may be time-consuming due the large volume of simulation data, but EMI prediction is more accurate than the frequency domain. An accurate EMI prediction requires extracting parasitic elements of the converter components and PCB. Parasitic values and characteristics of the passive and active components, in addition to PCB trace parameters, are necessary to investigate conducted EMI for power electronics systems. For instance, the equivalent series inductance (ESL) and resistance (ESR) of the output capacitor attenuate the capacitor effectiveness in high frequencies and should be included in the EMI model. In addition, cross-coupling capacitances of the transformer between the primary and secondary windings serve as a path for CM-EMI [15]. In addition, unwanted resonances between transformer capacitances and the leakage inductor (L_{lk}) contribute to EMI. The measured values of cross-coupling capacitances and leakage inductances using an LCR meter are included in the transformer model, as shown in Table 1. Since the major parasitic capacitance contributing to CM-EMI is the drain-to-earth capacitance (C_{DE}), it is measured to model the CM-EMI, in addition to other parasitic capacitances between diodes and the earth. The measured C_{DE} is around 10 pF with ungrounded heat sink. For active components, OrCAD software models are used, which consist of several parasitic parameters such as the MOSFET output capacitance.

To model the conducted EMI propagation path, PCB trace parameters should be extracted [11]. The resistance and inductance of each trace are measured via an LCR meter to construct the EMI model of the converter. To avoid complicated circuit models and extensive calculations, the coupling between traces and the trace capacitance is ignored. Finally, the EMI model of the converter is extracted. The derived model of the primary side is shown in Figure 2. In this figure, L_{Ti} and R_{Ti} represent the inductance and resistance of trace i, respectively.

2.2. Simulation model of EMI measurement setup

For conducted EMI measurement, a line impedance stabilization network (LISN) is used to present specified impedance over the frequency of interest [16]. LISNs according to CISPR Standard 22 are inserted between each input line and the power converter to perform the conducted EMI test. To distinguish between CM and DM conducted emissions, a differential-mode rejection network (DMRN) is connected to the input port of the spectrum analyzer for CM emissions measurement [17]. The simulation models of LISNs and the DMRN are shown in Figure 3. The spectrum analyzer port is modeled by a 50 Ω resistor, as illustrated in Figure 3.

Further for the converter EMI model, the measurement network model is implemented in OrCAD. The step time during regular OrCAD simulation is variable. Thus, LabVIEW is used to fix the step time for better frequency spectrum analysis. In addition, the resolution bandwidth (RBW) of the spectrum analyzer model can be set according to CISPR Standard 22 [10]. Figure 4 shows the block diagram of the simulation procedure to predict the conducted CM-EMI. According to Figure 4, the voltage across the DMRN (positive line side) is exported from OrCAD to LabVIEW software. FFT is utilized to predict the conducted EMI in LabVIEW. The prediction results of CM emissions in 100–150 kHz and 150 kHz–30 MHz frequency ranges are shown in Figure 5. Since EMC standards define emission limits in dBmu V, the EMI levels unit is converted to dBmu V in LabVIEW to compare it with the EMC standard limit. According to Figure 5, the main EMI peak at 130 kHz switching frequency is 64.5 dBmu V and around 81.5 dBmu V in the 150 kHZ–30 MHz frequency band.

3. Measurement results of conducted CM-EMI

In order to verify EMI prediction results, experimental results are presented in this section. The switch voltage and current waveforms of the converter prototype with reset winding are shown in Figure 6. There are

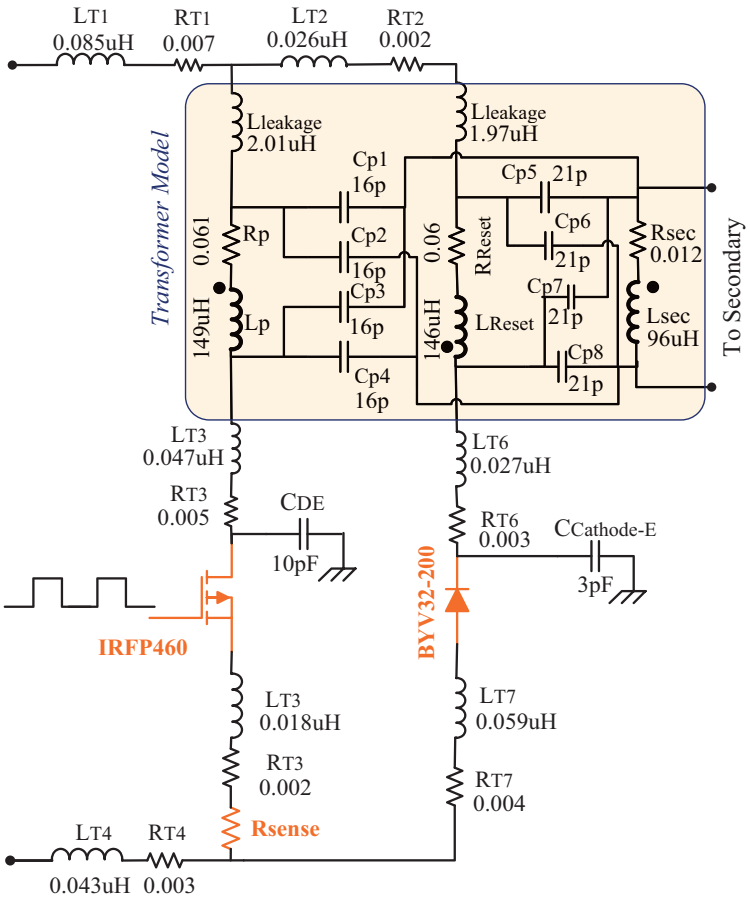

Figure 2. Derived EMI model (primary side) of the forward converter in the case of ungrounded heat-sink (low C_{DE}).

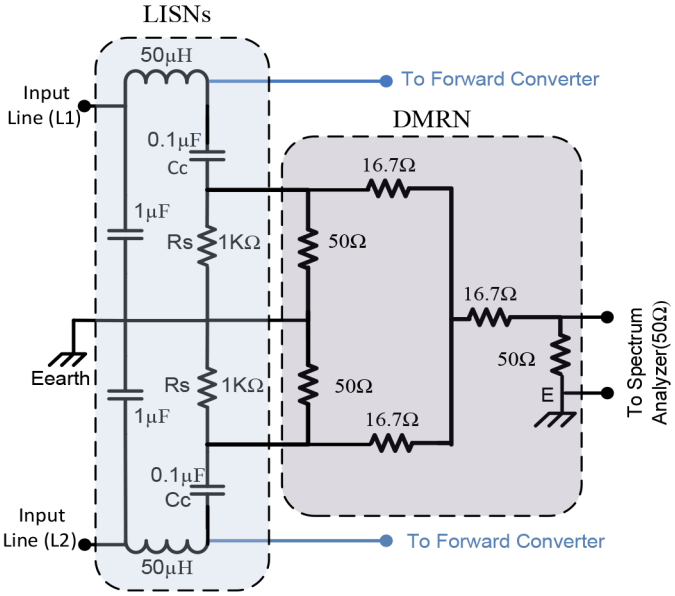

Figure 3. LISNs and DM rejection network (DMRN).

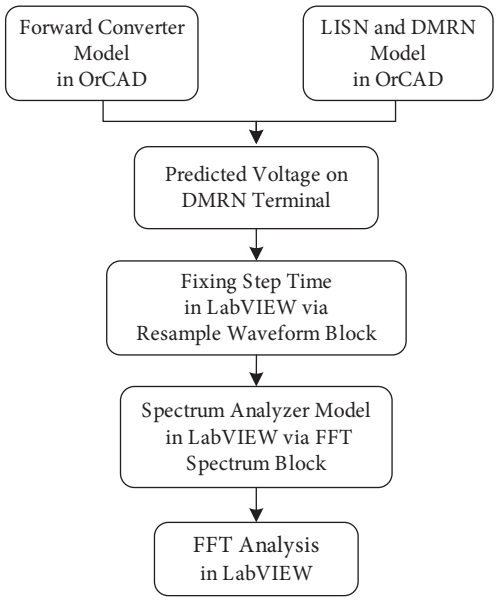

Figure 4. Conducted CM-EMI prediction procedure.

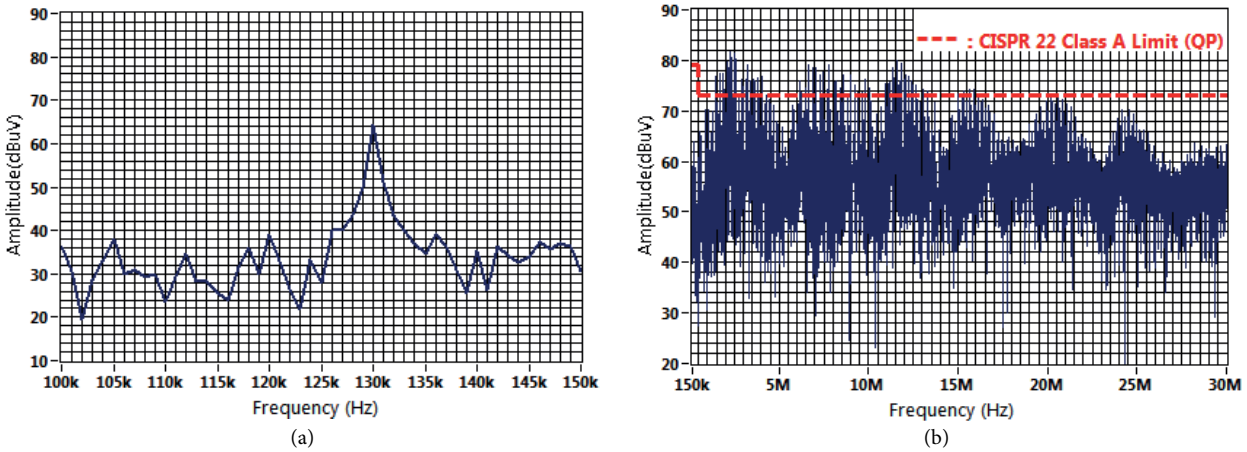

Figure 5. CM-EMI simulation results of forward converter with reset winding (in the case of low C_{DE} (10 pF): a) vertical axis: 10–90 dBmu V, horizontal axis: 100–150 kHz; b) vertical axis: 20–90 dBmu V, horizontal axis: 0.15–30 MHz.

considerable voltage and current spikes due to the existence of parasitic elements, which lead to electromagnetic interference as seen in the simulation results. For instance, the resonance between the switch output capacitor and transformer leakage inductance causes a voltage spike at the turn-off instant, as shown in Figure 6. In addition to the converter prototype, CISPR 22 LISNs and DMRN, shown in Figure 3, are built to establish conducted common-mode EMI measurement. The DMRN output terminal is connected to the input port of a HAMEG spectrum analyzer. The resolution bandwidth (RBW) is set to 1 kHz for 100–150 kHz and 10 kHz for 150 kHz–30 MHz. The measurement results are shown in Figure 7, in addition to CISPR 22 (Class A: Quasi Peak) and FCC limits.

The experimental results show that the EMI main peak reaches 62 dBmu V in the 100–150 kHz frequency band and 76 dBmu V at 6.8 MHz in the 150 kHz–30 MHz frequency band. Compared to the simulation results,

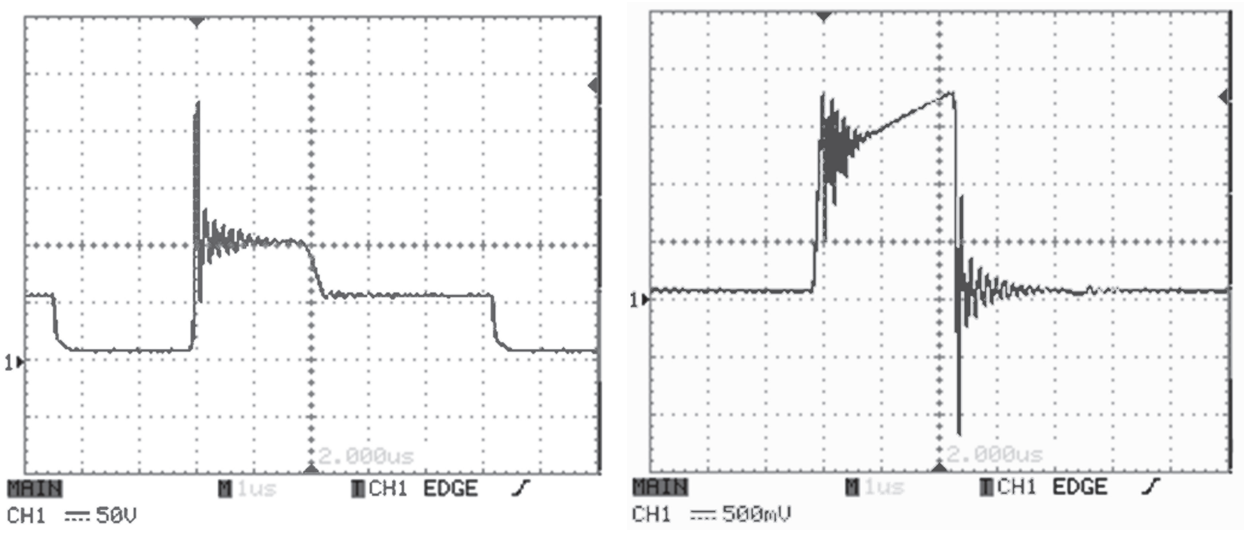

(a) (b)

Figure 6. Experimental waveforms of the forward converter with reset winding: a) switch voltage, vertical axis: 50 V/div., horizontal axis: 1 *mu* s/div; b) switch current, vertical axis: 0.5 A/div., horizontal axis: 1 *mu* s/div.

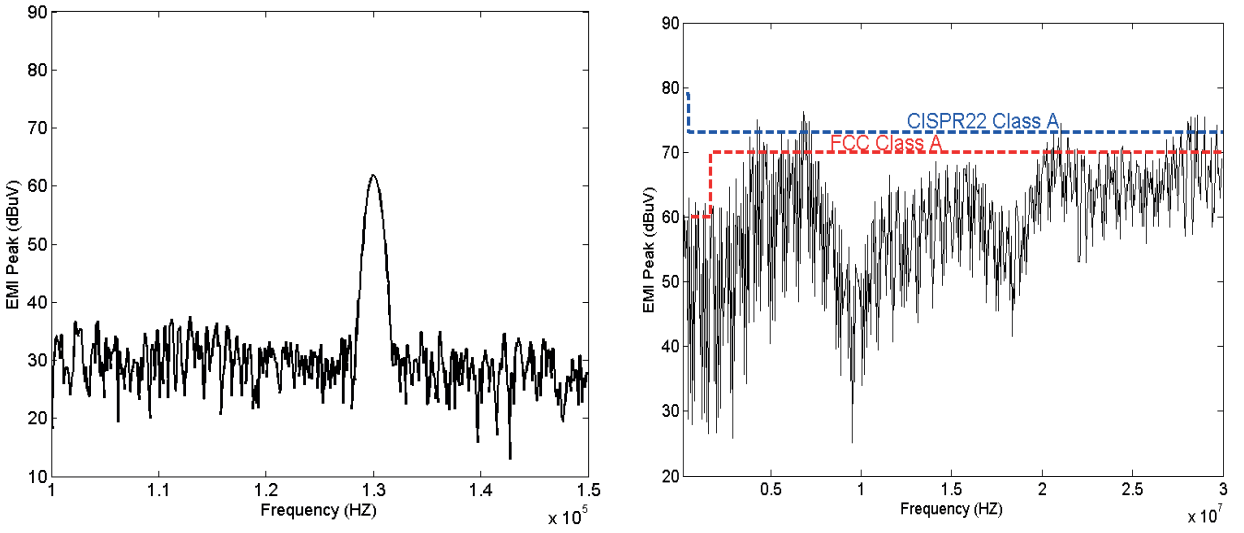

(a) (b)

Figure 7. CM-EMI experimental results of forward converter with reset winding: a) vertical axis: 10–90 dB*mu* V, horizontal axis: 100–150 kHz; b) vertical axis: 20–90 dB*mu* V, horizontal axis: 0.15–30 MHz.

the main EMI peak at 130 kHz is predicted with around 4% error, while the prediction error is around 7% for the maximum EMI peak located in the 150 kHz–30 MHz frequency band. The comparison between prediction and measurement results for various frequency ranges is shown in Figure 8, which verifies that the derived EMI model properly predicts the EMI levels of the forward converter with reset winding. Differences are due to ignoring some parameters such as LISN and DMRN parasitic traces, cable losses, and the coupling between PCB traces.

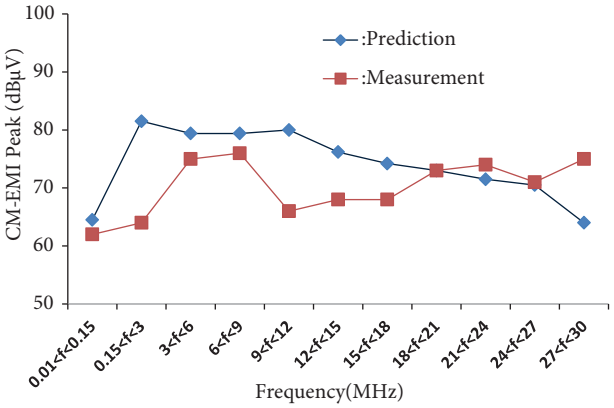

Figure 8. Comparison between prediction and measurement results of conducted CM-EMI (forward converter with reset winding).

4. CM-EMI comparison between various core-reset methods

In addition to the reset winding scheme, the RCD clamp scheme is implemented in the forward converter to evaluate its effects on the conducted CM-EMI. In addition to simplicity, another benefit of the RCD reset circuit is that a maximum duty cycle of more than 50% can be achieved with lower MOSFET voltage stress with respect to the reset winding method. However, an RCD clamp circuit can decrease the efficiency of isolated pulse-width modulation (PWM) DC-DC converters, such as forward converters [18]. Since the energy of magnetizing and primary leakage inductors in a switching cycle is dissipated in the RCD circuit, the following equation can be written [19]:

$$R_{RCD} = \frac{V_R^2}{\left[\frac{1}{2}L_m I_{L_m}^2 + \frac{1}{2}L_{LK}(I_{L_m} + nI_O)^2\right].f_{sw}}, \tag{1}$$

where L_m is the magnetizing inductance, L_{LK} is the transformer leakage inductance, n is the transformer ratio, I_O is the converter output current, and V_R is the ripple voltage across the R-C branch, which can be expressed by:

$$V_R = \frac{\bar{D}V_{in}}{(1-\bar{D})}. \tag{2}$$

Assuming 10% ripple for the capacitor voltage, the capacitor value is determined based on the discharge time (Δt) [19]. For a 33% duty cycle, the calculated values of the resistor and capacitor are around 300 Ω and 210 nF, respectively. Further for the RCD reset method, a zener diode clamp is implemented in the forward converter prototype. CM electromagnetic emissions of the forward converter with RCD and zener diode methods are measured, as shown in Figure 9.

The comparison between CM-EMI levels of the forward converter with mentioned passive core-reset methods are illustrated in Figure 10 for various frequency ranges. Considering the full frequency band, it can be seen that although the reset winding approach offers the benefit of lowest dissipation, the RCD reset method has generally better performance from an EMC standpoint than the reset winding and zener diode methods, especially below 18 MHz.

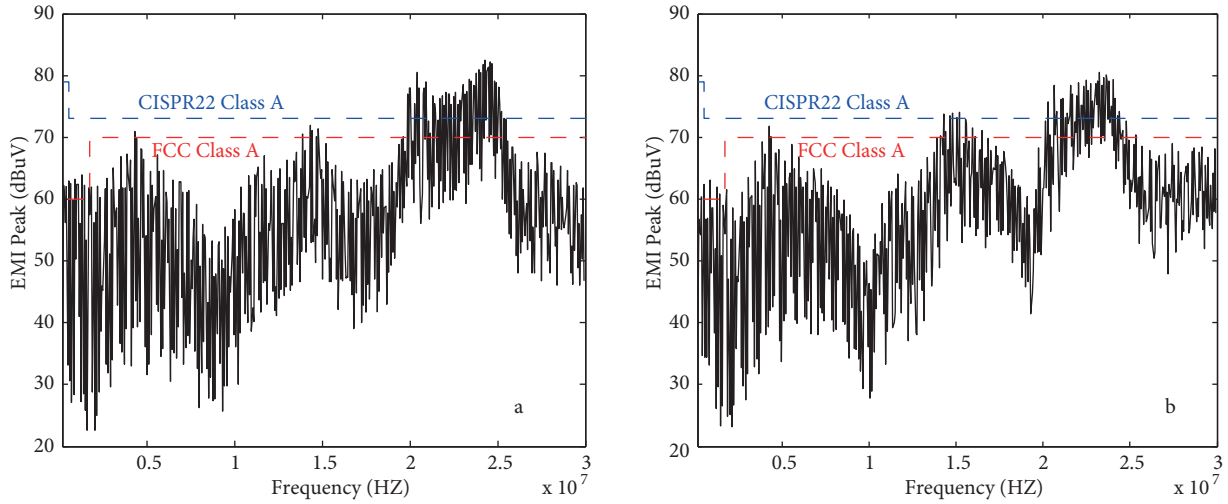

Figure 9. CM-EMI experimental results of forward converter with passive reset schemes: a) RCD clamp; b) zener diode clamp. Vertical axis: 20–90 dBmu V, horizontal axis: 0.15–30 MHz.

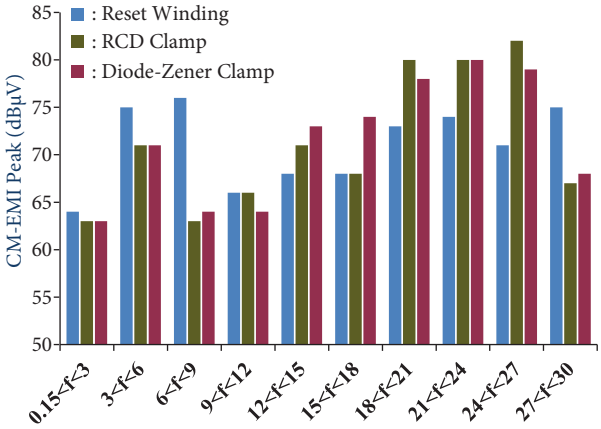

Figure 10. CM-EMI comparison of the passive core-reset schemes.

According to Figure 10, CM-EMI for the converter with reset winding in 150 kHz–9 MHz and 27–30 MHz frequency ranges is greater than in the other 2 cases. Unexpected couplings and leakage inductances can be mentioned as the reason. For the CM-EMI peak at 130 kHz switching frequency, passive core-reset has a similar result.

Low-side and high-side active clamps, which are used to reduce switch stress, are also implemented in the forward converter to evaluate their effects on conducted CM emissions. Clamp capacitor, the C_{CL} value, is calculated such that the resonant time between C_{CL} and magnetizing inductance is much greater than the maximum turn-off time [4]. Consequently, the selected C_{CL} value is 330 nF by the following equation, which is valid for both the high-side and low-side active clamp circuits:

$$C_{CL} \geq \frac{10.(1\text{-}\underline{D})}{L_m.(2\pi f_{sw})}. \tag{3}$$

The comparisons between CM-EMI experimental results of the forward converter with low-side and high-side active clamps are illustrated in Figure 11, in addition to the RCD reset scheme. The high-side clamp has more

conducted CM-EMI. This could be due to more parasitic elements and resonances, which are related to the loop of C_{CL}, clamp switch, and the transformer leakage inductance in Figure 1d. The low-side active clamp, which is employed across the main switch, has the best performance for CM-EMI reduction with respect to the passive reset schemes and low-side active clamp. The loss, switch stress [2,19], and cost parameters, in addition to the EMI, are compared in Table 2 for the single-switch forward converter.

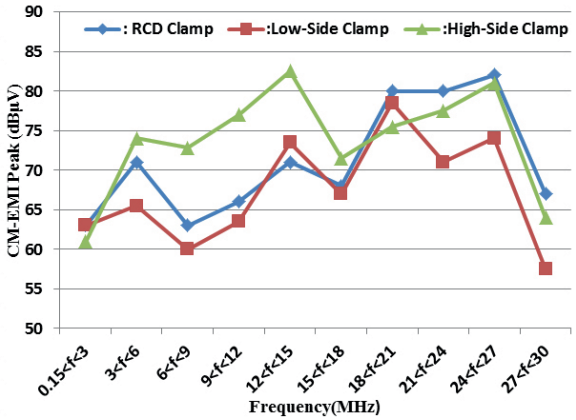

Figure 11. Comparison between CM-EMI levels of the active reset schemes and RCD clamp.

Table 2. Loss, cost, switch stress, and conducted EMI comparison.

Core-reset method	Low loss	Low cost	Low stress	Low EMI
Reset winding	+	+		
RCD clamp		+ +	+	+
Zener diode clamp		+	+	
High-side clamp	+ +		+ +	
Low-side clamp	+ +		+ +	+ + +

5. Conclusion

In this paper, the conducted common-mode EMI of a forward converter was predicted considering the main parasitic elements and PCB traces without a complicated model. To simulate CM emissions, LISNs and DMRN were modeled. The experimental results verified that the presented EMI model predicts EMI peaks with acceptable error, especially for the main EMI peak at 130 kHz (f_{sw}) and the 150 kHz–30 MHz frequency band. To select the proper core-reset method from an EMC standpoint, CM emissions of conventional passive and active core-reset techniques were compared. Considering passive schemes, the RCD clamp almost yielded lower conducted CM-EMI levels, especially below 18 MHz. Furthermore, the experimental results for the forward converter with high-side and low-side active clamps illustrated that the low-side active clamp has the best performance from the EMC standpoint, in addition to low losses and switch stress.

References

[1] Park KB, Moon GW, Youn MJ. Series-input series-rectifier interleaved forward converter with a common transformer reset circuit for high-input-voltage applications. IEEE T Power Electr 2011; 26: 3242-3253.

[2] Tan FD. The forward converter: from the classic to the contemporary. In: IEEE 2002 Applied Power Electronics Conference; 10–14 March 2002; Dallas, TX, USA. Piscataway, NJ, USA: IEEE. pp. 857-863.

[3] Adib E, Farzanehfard H. Analysis and design of a zero-current switching forward converter with simple auxiliary circuit. IEEE T Power Electr 2012; 27: 144-150.

[4] Açık A, ÇadırcıI. Active clamped ZVS forward converter with soft-switched synchronous rectifier. Turk J Electr Eng Co 2002; 10: 473-491.

[5] Çoban A, Çadirci I. Active clamped two-switch forward converter with a soft switched synchronous rectifier. IET Power Electr 2011; 4: 908-918.

[6] Wu HF, Xing Y. A family of forward converters with inherent demagnetizing features based on basic forward cells. IEEE T Power Electr 2010; 24: 2828-2834.

[7] Kim JK, Choi SW, Moon GW. Zero-voltage switching postregulation scheme for multioutput forward converter with synchronous switches. IEEE T Ind Electron 2011; 58: 2378-2386.

[8] Yazdani MR, Farzanehfard H, Faiz J. EMI analysis and evaluation of an improved ZCT flyback converter. IEEE T Power Electr 2011; 26: 2326-2334.

[9] Bishnoi H, Mattavelli P, Burgos R, Boroyevich D. EMI behavioral models of DC-fed three-phase motor drive systems. IEEE T Power Electr 2014; 29: 4633-4645.

[10] IEC International Special Committee on Radio Interference (CISPR). Information Technology Equipment—Radio Disturbance Characteristics—Limits and Methods of Measurement. Publication 22. Geneva, Switzerland: IEC, 1997.

[11] Yazdani MR, Farzanehfard H. Conducted electromagnetic interference analysis and mitigation using zero-current transition soft switching and spread spectrum techniques. IET T Power Electr 2012; 5: 1034-1041.

[12] Kong P, Jiang Y, Lee FC. Common mode EMI noise characteristics of low-power AC–DC converters. IEEE T Power Electr 2012; 27: 731-738.

[13] Çabuk G, Kılınç S. Reducing electromagnetic interferences in flyback AC–DC converters based on the frequency modulation technique. Turk J Electr Eng Co 2012; 20: 71-86.

[14] Pressman AI, Billings K, Morey T. Switching Power Supply Design. 3rd ed. New York, NY, USA: McGraw-Hill, 2009.

[15] Fu D, Wang S, Kong P, Lee FC, Huang D. Novel techniques to suppress the common-mode EMI noise caused by transformer parasitic capacitances in DC–DC converters. IEEE T Ind Electron 2013; 60: 4968-4977.

[16] Chittibabu KK, Alphonse NK. Analysis of conducted EMI with a standalone solar-powered DC motor. Turk J Electr Eng Co 2013; 21: 1260-1271.

[17] Ott HW. Electromagnetic Compatibility Engineering. Hoboken, NJ, USA: John Wiley & Sons, 2009.

[18] Aksoy I. A new PSFB converter-based inverter arc welding machine with high power density and high efficiency. Turk J Electr Eng Co 2014; 22: 1501-1516.

[19] Choi HS. Design guidelines for off-line forward converters using Fairchild power switch. Fairchild Semiconductor Application Note AN4134. San Jose, CA, USA: Fairchild, 2004.